

Submitted by
Benjamin Schmid Ties

Submitted at
Faculty of Engineering

Supervisor
Prof. Petti

July 2025

Design of a Wearable Screen-Printed DC System for Iontophoretic Sweat Extraction in Biomedical Applications



Bachelor Thesis
Faculty of Engineering

**FREE UNIVERSITY OF
BOZEN-BOLZANO**
Bruno Buozzi Str. 1
39100 Bozen-Bolzano, Italy
www.unibz.it

Declaration

I hereby declare and confirm that this thesis is entirely the result of my own original work. Where other sources of information have been used, they have been indicated as such and properly acknowledged. I further declare that this or similar work has not been submitted for credit elsewhere. The copy at hand is identical to the electronically submitted document.

Bozen-Bolzano, on 9th July, 2025

Benjamin Schmid Ties

Acknowledgements

I would like to express my deepest gratitude to Prof. Luisa Petti for supervising my thesis and for her continued support throughout the entire course of my studies at the Free University of Bolzano. I am especially thankful to her and to Moritz Ploner, a PhD student in her group, for setting up the thesis topic and providing the initial problem statement, which laid the foundation for this work. Moritz's expertise in wearable biosensors was particularly valuable in shaping the direction of my project. I also sincerely thank Dr. Arvind Gurusekaran and Dr. Giulia Elli, two postdocs in the group of Prof. Petti, for their generous assistance in the lab. Their help in preparing the materials and devices, as well as in carrying out the measurements, was crucial to the progress of this thesis. I truly appreciate the many hours we spent working together and their willingness to share their knowledge and time.

Abstract

This thesis presents the design, fabrication, and testing of a screen-printed DC system for iontophoretic sweat extraction, with applications in wearable biosensing devices. The system was developed using thermoplastic polyurethane (TPU) as a flexible substrate and silver/silver chloride (Ag/AgCl) as electrode material due to its biocompatibility and widespread clinical use. Screen printing was used to fabricate elliptical electrodes optimized for skin contact, and Strat-M® synthetic membrane was employed as a substitute for human skin during experiments. First, the performance of the printed electrodes was evaluated through optical inspection using microscopy, four-point probe measurements of sheet resistance, and optical profilometry. The printed electrodes yielded an average sheet resistance of $44.47 \frac{m\Omega}{sq}$ with a standard deviation of $10.57 \frac{m\Omega}{sq}$. Subsequently, a test platform was developed to simulate iontophoresis-driven ion transport across the membrane, using artificial sweat as the source medium. Ionic permeation was analyzed via cyclic voltammetry, confirming successful ion transfer under various current intensities (0.1 mA, 0.2 mA, 0.3 mA). These preliminary results pave the way towards more user-friendly and non-invasive wearable devices for continuous health monitoring.

Kurzfassung

Diese Facharbeit stellt die Entwicklung, Herstellung und Validierung eines durch Siebdruck hergestellten Gleichstromsystems zur Schweißextraktion durch Iontophorese zur Verwendung in tragbaren Systemen vor. Das System wurde unter Verwendung von thermoplastischem Polyurethan (TPU) als flexiblem Substrat und Silber/Silberchlorid (Ag/AgCl) als Elektrodenmaterial entwickelt. TPU wurde wegen seiner hohen Verformbarkeit als Substrat gewählt. Ag/AgCl wurde wegen der guten elektrischen Eigenschaften, Biokompatibilität und Verformbarkeit gewählt. Für die durchgeführten Experimente diente die Strat-M® Membran als Ersatz für menschliche Haut. Die Leistung der gedruckten Elektroden wurde mittels optischer Inspektion unter dem Mikroskop, Vier-Punkt-Messungen des Flächenwiderstands und optischer Profilometrie bewertet. Der durchschnittliche Flächenwiderstand betrug $44.47 \frac{m\Omega}{sq}$ mit einer Standardabweichung von $10.57 \frac{m\Omega}{sq}$. Eine Testplattform wurde entwickelt, um den durch Iontophorese beschleunigten Ionentransport über die Membran zu simulieren, wobei künstlicher Schweiß als Quelle verwendet wurde. Die Ionenpermeation wurde mittels zyklischer Voltammetrie analysiert, wobei ein erfolgreicher Ionentransfer bei unterschiedlichen Stromstärken (0.1 mA, 0.2 mA, 0.3 mA) bestätigt wurde. Diese vorläufigen Ergebnisse bahnen den Weg für benutzerfreundlichere und nicht-invasive tragbare Geräte zur kontinuierlichen Gesundheitsüberwachung.

Sintesi

Questa tesi presenta la progettazione, la fabbricazione e la validazione di un sistema a corrente continua serigrafato per l'estrazione del sudore tramite ionoforesi, con applicazioni nei dispositivi indossabili per il biosensing. Il sistema è stato sviluppato utilizzando poliuretano termoplastico (TPU) come substrato flessibile e argento/cloruro d'argento (Ag/AgCl) come materiale per gli elettrodi, poiché biocompatibile e ampiamente utilizzato in ambito clinico. La serigrafia è stata impiegata per realizzare elettrodi ellittici ottimizzati per il contatto con la pelle, mentre la membrana sintetica Strat-M® è stata utilizzata come sostituto della pelle umana. Le prestazioni degli elettrodi stampati sono state valutate tramite ispezione ottica al microscopio, misurazioni a quattro punte della resistenza superficiale e profilometria ottica. La media delle resistenze superficiali degli elettrodi è $44.47 \frac{m\Omega}{sq}$ con una deviazione standard di $10.57 \frac{m\Omega}{sq}$. Inoltre, è stata sviluppata una piattaforma di test per simulare il trasporto ionico attraverso la membrana, indotto da ionoforesi, utilizzando sudore artificiale come mezzo di origine. È stato possibile confermare il trasferimento di ioni a diverse intensità di corrente (0.1 mA, 0.2 mA, 0.3 mA), analizzando la permeazione ionica mediante voltammetria ciclica. Questi risultati preliminari rappresentano un passo importante verso lo sviluppo di dispositivi indossabili sempre più discreti e non invasivi, pensati per un monitoraggio continuo della salute.

Contents

Declaration	ii
Acknowledgements	iii
Abstract	iv
Kurzfassung	v
Sintesi	vi
1 Introduction	1
1.1 Motivation	1
1.2 State of the art	2
1.3 Objectives	3
1.4 Applications	4
2 Materials and methods	5
2.1 System overview	5
2.2 Materials	6
2.2.1 Substrate: TPU	6
2.2.2 Electrode material: Ag/AgCl	6
2.2.3 Artificial sweat	7
2.2.4 Synthetic model for human skin: Strat-M®	7
2.3 Electrode design and fabrication	8
2.3.1 Electrode design	8
2.3.2 Electrode screen printing	9
2.4 Characterization of electrodes	10
2.4.1 Visual inspection by microscope	10
2.4.2 Sheet resistance measurements	10
2.4.3 Characterization of surface roughness by optical profilometry	11
2.5 Test setup	11
2.5.1 Design and assembly	11
2.5.2 Procedure	12
2.6 Monitoring ionic permeation through synthetic membrane	13
2.6.1 Cyclic voltammetry	13
2.6.2 Parameters for cyclic voltammetry	15
3 Results	17
3.1 Performance evaluation of screen-printed Ag/AgCl electrodes on TPU substrate	17
3.1.1 Sheet resistance	17
3.1.2 Visual inspection with microscope	18
3.1.3 Evaluation of surface roughness with optical profilometer	19
3.2 Determination of current intensity for optimal ion transfer	20
3.2.1 Processing of measurements	20
3.2.2 Analysis of measurements	21
4 Conclusion	23
References	24

1

Introduction

1.1 Motivation

The demand for wearable devices for continuous health monitoring has dramatically increased in recent years [1]. Electrical and mechanical biosignals, such as muscle electrical activity or blood pressure, are commonly used to assess a patient's physiological state via wearable technologies [2]. In contrast, monitoring of biochemical profiles, even though they can provide valuable insights into the patient's health state, often requires laboratory equipment or point-of-care testing and has not yet been widely integrated into wearable devices. While blood has been considered the standard for medical monitoring of biomarkers [3], it is not ideal for many patient groups, such as newborns, the elderly, or hemophagic individuals. On the other side, alternative bodily fluids such as urine, tears, and saliva are often impractical or unavailable for biomarker detection [4]. Sweat, in comparison, is rich in analytes [5], that provide valuable insight into the body's physiological state and is available almost everywhere on the body, making it an ideal basis for analysis using wearable biosensors [6]. These analytes include electrolytes, metabolites, hormones, peptides, and proteins [7]. The concentration in blood of many of these analytes is highly correlated with the levels in sweat [8]. Wearable biosensing technologies, including optical biosensors [9, 10], colorimetric assays [11], and electrochemical sensing platforms [12, 13, 14], have shown promising results for noninvasive health monitoring. However, their effective on-body deployment is often limited by the sporadic and unpredictable nature of sweat secretion, which hinders their ability to deliver continuous and reliable data [6]. Sweat is produced in sweat glands, which can be subdivided into different types: the eccrine, apocrine, and apoeccrine glands [15]. The apocrine and apoeccrine glands are less relevant in the context of wearable biosensors, as they play a smaller role in sweat production. Currently, most wearable biosensors rely on passive sweat extraction, which is limited to certain physiological and environmental conditions [16]. Since its primary function is thermoregulation, sweat is not readily available in sedentary individuals or in climate-controlled environments [17]. Therefore, a system capable of extracting sweat

on demand is needed for reliable, continuous analysis. A method often used for this task is iontophoresis [17]. Iontophoresis is an active and non-invasive method for extracting sweat that uses a small electric current to transfer cholinergic agents like pilocarpine [18] or carbachol into the skin, which stimulates local sweat production in the eccrine sweat glands [19]. More generally, iontophoresis can be used to facilitate ion transfer across a membrane using an electric field [20]. This thesis on the design of a wearable, screen-printed direct current iontophoretic system addresses a fundamental challenge in the broader context of sweat-based wearable biosensors. The reliable and controlled extraction of sweat for continuous biomarker analysis is a problem that has received much attention but has not yet been fully solved [21]. Specifically, the use of synthetic membranes such as Strat-M® to model skin behavior during iontophoresis remains largely unexplored. Moreover, key parameters like the density and duration of iontophoresis current lack clear definition in the literature, highlighting the need for further research.

1.2 State of the art

Multiple approaches to extracting sweat from the skin through iontophoresis have been developed in the past decade. As shown in [22], self-powered designs that do not rely on an external power source are possible. To power the device, a bismuth telluride (Bi_2Te_3) based thermoelectric generator (TEG) was implemented. In very hot environments, where the difference in temperature between the human skin and the external environment is less than 6 °C, the Bi_2Te_3 based TEG does not generate sufficient power. The authors worked around this by using a Li-ion battery that keeps the device functional when the TEG alone is insufficient [22]. The device constructed by the authors includes a microfluidic layer to provide a well-defined path for sweat extracted through iontophoresis. The cholinergic agent carbachol is delivered, which triggers sudomotor axon reflexive sweating on command. A direct current of 0.2 mA was applied for 10 minutes, which was found to be most efficient. At higher currents, the increase in sweat production was not significant. With the applied current of 0.2 mA, a prolonged sweat response could be triggered (8 hours). The iontophoresis electrode design including a biosensor array is shown in figure 1.1(b) [22].

In [23], a method has been proposed that enables uniform mass production of sensing patches. Using a roll-to-roll process, the authors were able to achieve a throughput of 60 devices per minute. It was found that when delivering the cholinergic agent pilocarpine through iontophoresis, sweating is stimulated within 3 minutes, which enables real-time detection of biomarkers [23]. Also, it could be demonstrated that local and whole-body fluid loss are highly correlated, which makes it possible to track hydration status.

Simultaneous extraction of both interstitial fluid (ISF) and sweat has been achieved through dual iontophoresis [24]. The proposed dual iontophoretic system is able to combine ISF

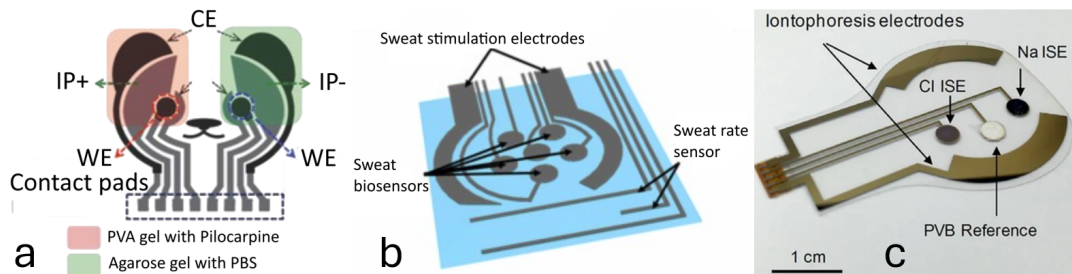


Figure 1.1: Overview of state of the art wearable devices for sweat extraction and sensing. (a) Dual iontophoresis design for simultaneous extraction of sweat and interstitial fluid (adapted from [24]; IP=iontophoresis; WE/CE=working/counter electrode); (b) Iontophoresis electrodes and biosensor array for self-powered device (adapted from [22]); (c) Iontophoresis electrodes and biosensors on PET substrate [17].

and sweat extraction by extracting ISF at the cathode and delivering the sweat-inducing agent pilocarpine at the anode. The wearable device is shown in figure 1.1(a) [24]. The two primary mechanisms used to achieve the simultaneous extraction are: (1) electrorepulsion: positively charged cations of the cholinergic agent pilocarpine are repelled from the anode, and (2) electroosmosis: a convective flow, which includes uncharged molecules like urea and glucose induced by the current from the anode to the cathode [1]. In [17], a design based on Polyethylene terephthalate (PET) treated with isopropyl alcohol and O₂ plasma etching was proposed. The electrode shape was patterned via photolithography and coated with 30/100 nm of chromium and gold. The outer electrodes were used to deliver cholinergic agonists into the skin, which stimulate sweat secretion. The iontophoresis current was controlled by a voltage-controlled current source, which itself was controlled by a pulse-width-modulated (PWM) signal emitted by a standard microcontroller. The system is shown in figure 1.1(c) [17].

Other iontophoretic systems, like the one proposed in [25], use a tattoo-based wearable device. Similar to the other devices presented, sweat is induced by delivering pilocarpine transdermally. The electrodes were screen-printed onto a wearable temporary-tattoo paper. Like in our design, the iontophoresis electrodes are based on Ag/AgCl. A common property of many state-of-the-art wearable iontophoresis systems is the elliptical spaced electrode design, shown in figure 1.1(a) and 1.1(b), which our design was inspired by.

1.3 Objectives

This thesis aims to address the gaps in the literature mentioned previously. Results are discussed in chapter 3.

1. Performance evaluation of screen-printed Ag/AgCl electrodes on TPU substrate
2. Determination of current intensity for optimal ion transfer

1.4 Applications

Recent advances in cutting-edge research have demonstrated the possibility for flexible platforms that can detect low concentration cytokines in sweat. These include critical inflammatory biomarkers like tumor necrosis factor-alpha (TNF- α) [12, 26], interleukin-6 (IL-6) [8, 27], which are essential for monitoring the immune response and the progression of certain diseases [28]. Their concentration in sweat is often highly correlated to their concentration in blood [29]. While state-of-the-art biosensors have demonstrated high sensitivity and selectivity for cytokine detection, a reliable sweat source is necessary for real-time and longitudinal monitoring. This thesis aims to establish a foundation for understanding the behavior of synthetic membranes, specifically Strat-M[®], under iontophoretic conditions, and to explore appropriate ranges of current density and duration for effective sweat stimulation. This thesis is part of a PhD research project conducted by Moritz Ploner from the Sensing Technologies Lab at the Free University of Bolzano. The results of this work will be integrated into the broader scope of that research in the future. These findings serve as an initial step toward the development of fully integrated wearable systems capable of overcoming the physiological and environmental limitations of passive sweat collection. Such groundwork is essential for translating the platform from lab-scale validation to practical diagnostic applications, which include cytokine detection but can be applied in the broader context of sweat sensing.

2

Materials and methods

2.1 System overview

The method used for extracting sweat from the skin is iontophoresis. In iontophoresis, a mild current is applied through the skin. In order to apply this current, flexible and wearable electrodes are needed that stay in contact with the skin. An elliptical design for the iontophoresis electrodes was chosen. The electrodes were screen-printed with Ag/AgCl ink on a TPU substrate using a semi-automatic screen-printing machine. The electrodes were characterized using sheet resistance measurements, visual inspection and optical profilometry. In order to conduct the experiments, a synthetic membrane, specifically Start-M®, was used instead of human skin for repeatable and safe testing. The membrane is designed for use in a Franz-Diffusion-Cell, a lab instrument made for testing the permeability of membranes that allows the placement of a membrane in between donor and receptor chambers. The donor and receptor chambers contain solutions with high and low ion concentrations, respectively. The ions contained in the donor solution permeate through the membrane at a rate predictive of the permeation through human skin. In our case, the donor solution used was artificial sweat and the receptor solution was distilled water. We designed and built a setup that works similarly to a Franz-Diffusion-Cell but allows placing iontophoresis electrodes in contact with a synthetic membrane and the connection of a current source. To measure ionic permeation through the membrane from the donor to the receptor chamber, various current intensities were applied through the electrodes and samples from the receptor chamber were taken at regular time intervals and analyzed using cyclic voltammetry.

2.2 Materials

2.2.1 Substrate: TPU

TPU was chosen as the substrate material for the iontophoresis electrodes. In the context of wearable devices, TPU offers several advantages compared to other materials commonly used in printed electronics, such as PET. The Young's modulus is a measure of the elasticity of a material, defined as

$$E = \frac{\sigma}{\epsilon} [\text{Pa}]$$

where σ is the stress in Pa and ϵ is the relative elongation $\epsilon = \frac{\Delta L}{L_0}$. The Young's modulus for different materials is shown in table 2.1. Compared with other polymers, TPU has a

Table 2.1: Young's modulus for flexible substrates [30]

Material	Young's Modulus [MPa]
TPU	7
Polyimide (PI)	2.5×10^3
PET	$2-4.1 \times 10^3$
Polycarbonate (PC)	$2-2.6 \times 10^3$
Polyethylene naphthalate (PEN)	$0.1-0.5 \times 10^3$
Polydimethylsiloxane (PDMS)	1

very low Young's modulus, making it very flexible and elastic. This property allows the electrodes to deform as needed while remaining in contact with the skin. Another important property for wearable devices is breathability [31]. Wearables that are not breathable can cause discomfort and/or irritation over time, as sweat accumulates between the skin and the device without evaporating [32]. Through electrospinning, TPU can be produced with fibrous pores, which allow high breathability [33].

2.2.2 Electrode material: Ag/AgCl

Silver/ silver chloride (Ag/AgCl) is one of the most commonly used materials for clinical electrodes and is thus ideal for use in wearable devices. Silver also reduces microbial growth, which improves hygiene and greatly reduces the risk of microbial infections [34]. When deposited as a thin layer on the TPU substrate, the material remains flexible. We observed that when the underlying TPU fabric was stretched beyond a certain point, visible cracks in the deposited Ag/AgCl began to form, greatly reducing or fully stopping electrical conductivity. In the experiments conducted, this was not critical because the electrodes remained stationary throughout the entire test. The specific silver/silver chloride paste used was the LOCTITE EDAG PE 409 E&C, which has a silver/silver chloride ratio of 9:1.

2.2.3 Artificial sweat

A test solution was prepared with components similar to real sweat. The solution was used to model the behavior of sweat permeating through the Strat-M® membrane. Six compounds were used to create the solution, including potassium chloride (KCl), sodium chloride (NaCl), creatinine, glucose, uric acid, and ascorbic acid.

Table 2.2: Artificial sweat components for 0.5 L total solution [35]

Component	Concentration [$\frac{mol}{L}$]	Molecular weight [$\frac{g}{mol}$]	Final mass [g]
KCl	0.016000	74.55130	0.59642
NaCl	0.060000	58.44000	1.75320
Creatinine	0.000168	113.1200	0.00950
Glucose	0.000340	180.4560	0.03068
Uric acid	0.000118	168.1103	0.00992
Ascorbic acid	0.000020	176.1200	0.00176

2.2.4 Synthetic model for human skin: Strat-M®

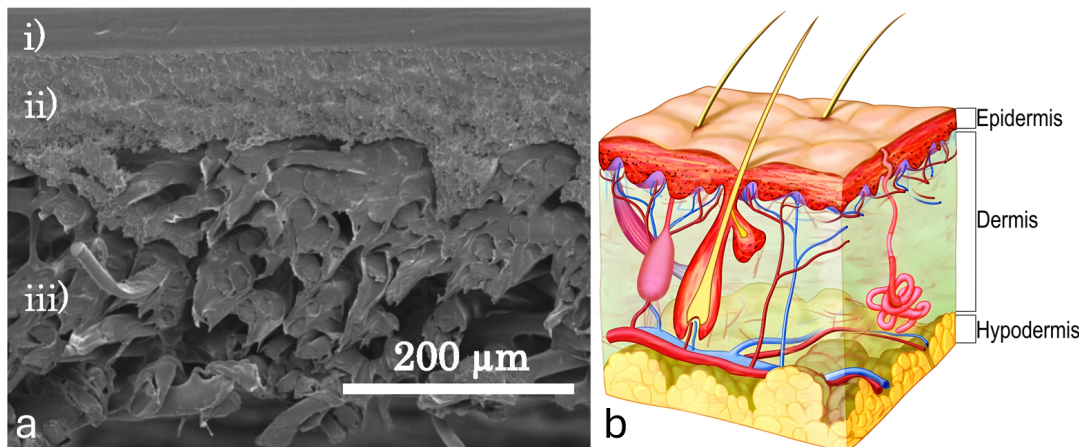


Figure 2.1: Strat-M® compared to human skin. (a) Scanning-electrode-microscope image of Strat-M® membrane [36] (i=epidermis, ii=dermis, iii=hypodermis); (b) Illustration of the three layers in human skin[37].

For the experiments conducted in this thesis, Strat-M® (Merck KGaA, Darmstadt, Germany) was used as a substitute for human skin. The synthetic membrane can serve as a model for transdermal diffusion and is therefore suitable for the experiments conducted. The membrane consists of two layers of polyester sulfone[36] and a layer of polyolefin, modeling various layers of the human skin. The permeability coefficients of various chemical compounds through the membrane are predictive of the permeability through human skin. An illustration of human skin and a scanning electron microscope image of Strat-M®

are shown side by side in figure 2.1. In figure 2.1(a), the different layers of the Strat-M® membrane are annotated. Here, i) corresponds to the epidermis, the two polyester sulfone layers denoted by ii) correspond to the dermis, and the polyolefin layer denoted by iii) corresponds to the hypodermis. The polyester sulfone layers provide resistance to drug permeation, and the polyolefin layer has wider pores and is more permeable. The polymeric layers are porous in structure and impregnated with synthetic lipids, which provide a gradient of pore size and diffusivity[38]. Strat-M® shows similar behavior to human skin, particularly for compounds with molecular weights in the range of 151 and 288 $\frac{g}{mol}$ [36]. Three out of the six compounds in the used formulation for artificial sweat from table 2.2 are contained in this range.

2.3 Electrode design and fabrication

2.3.1 Electrode design

For the iontophoresis-electrodes, an elliptical design was chosen. The wide elliptical area offers a large surface area for skin contact, with a centered recess allowing downstream placement of flexible biosensors, as shown in multiple state-of-the-art wearable designs in section 1.2. The design also contains square exposed pads connected to the elliptical electrodes, which allow the connection of a source meter. The high demands for current in iontophoresis require highly conductive paths. As initial results have shown, the narrow connections between the exposed pads and the iontophoresis electrodes were not conductive enough to support the current of 1 mA that was applied in the first experiments and were destroyed, as shown in section 3.1.1.

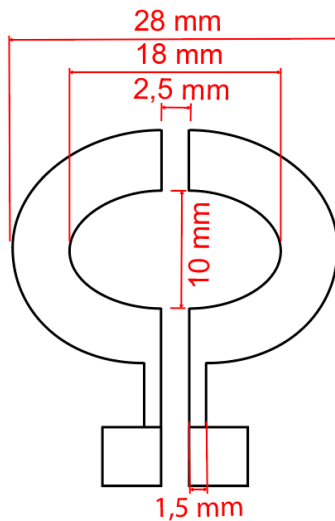


Figure 2.2: Design of iontophoresis electrodes including wide elliptical area for contact with human skin and square exposed pads that allow connecting a current source.

2.3.2 Electrode screen printing

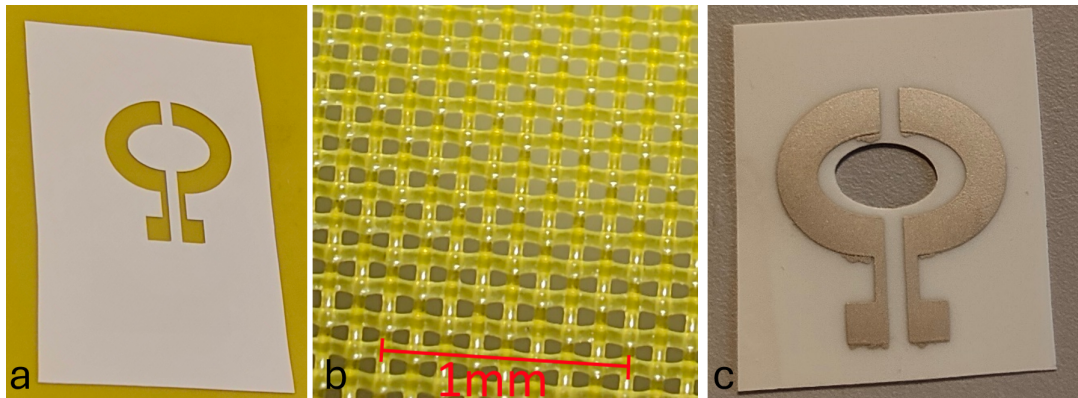


Figure 2.3: Screen printing overview. (a) Vinyl mask on polyester screen; (b) Polyester screen (close up) with mesh count 80 threads/cm; (c) Screen printed Ag/AgCl electrode after thermal curing.

The electrodes were fabricated using a semiautomatic screen printing machine (C920, Aurel S.p.A., Italy). Screen printing was chosen as a process for its low cost, scalability, and customizability. With screen printing, key parameters like substrate and print material, and coating thickness can be easily and quickly modified. First, a vinyl mask was fabricated using a laser cutter. The vinyl mask was then applied to a polyester screen, while being careful that it sits perfectly flat on the screen and making sure that there are no wrinkles or air pockets, as shown in figure 2.3(a). An important parameter in screen printing is the mesh count, which is crucial to the achievable resolution. A polyester screen with a mesh count of 80 threads/cm, shown in figure 2.3(b) was used, which is quite low but more than enough for the chosen design and size. The ink (LOCTITE EDAG PE 409 E&C) was then applied on top of the mask. The ink is designed specifically for use as an electrode material in medical sensing devices and offers easy printability. The machine has 2 squeegees; one (SG_1) is used to spread the ink onto the mask, and the other (SG_2) retrieves the ink to the initial position. During every iteration of the process, SG_1 is lowered to apply pressure to the screen and pulled across the mask, transferring the ink in the process. Afterwards, SG_1 is lifted and SG_2 is lowered, retrieving the ink back toward the initial location before the process starts over. An illustration of the screen printing process is shown in figure 2.4. During this process, the ink permeates through the pores of the screen onto the substrate. Over time, the quality of the mask degrades due to the friction applied by the squeegees, and it has to be replaced after roughly 10 iterations. After applying the ink to the substrate, the samples were transferred to an oven at 100 °C for 15 minutes to cure, ensuring that the ink turns solid and all of the solvent evaporates. A laser cutter was used to create an elliptical cutout between the electrodes, ensuring that this area on the Strat-M® membrane is in contact with the liquid in the receptor chamber of the Franz Diffusion Cell, as described in section 2.5.

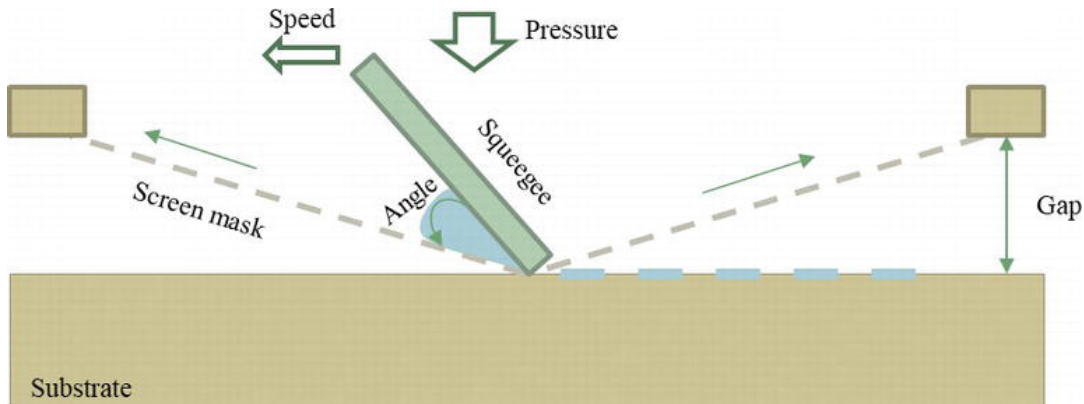


Figure 2.4: Illustration of screen printing process [39] with one squeegee. Ink (blue) permeates through the screen mask and coats the substrate.

2.4 Characterization of electrodes

2.4.1 Visual inspection by microscope

The screen-printed Ag/AgCl electrodes were visually inspected with an optical microscope (EZ4 E, Leica Microsystems Srl, Italy). Various defects were visible, caused by different problems in the screen printing process, as discussed in section 3.1.2. In a fully automated process, these defects can be avoided [23].

2.4.2 Sheet resistance measurements

The sheet resistance is a parameter that is often used to characterize materials of uniform thickness. The resistance of a conductor is generally expressed as $R = \rho \frac{L}{A} = \rho \frac{L}{Wt} [\Omega]$ where ρ is the resistivity of the material in $\Omega \frac{m^2}{m}$, L is the length in meters and A is the cross-sectional area in m^2 . The area is equal to $W \times t$ where W and t are the width and thickness of the conductor in meters. When the thickness is uniform, the parameter $\frac{\rho}{t} [\Omega]$, is also known as the sheet resistance $R_s [\frac{\Omega}{sq}]$. The unit $[\frac{\Omega}{sq}]$ is used to denote that a square conductor has constant resistance, regardless of its size, but the unit is dimensionally equal to ohms. To measure the sheet resistance of the fabricated electrodes, the four-point probe method was used. The specific device used was the Ossila Four-Point Probe. The manufacturer rates the device with an accuracy of $\pm 8\%$ and a precision of $\pm 3\%$ in the measurement range of our samples. Using this method, very high precision can be achieved. In four-point probes, a current is supplied through two probes, while voltage is measured with the remaining two probes. The advantage of this method is that the current supplied through the high-current path does not cause a voltage drop on the measurement wires and therefore does not impact the measurement directly. The sensing probes are connected to an ADC with high input impedance, such that a negligible current

flows through the wires. The voltage drop across the wires is then also negligible and therefore has no measurable impact on the measurement, reducing the bias. Numeric results are discussed in section 3.1.1.

2.4.3 Characterization of surface roughness by optical profilometry

The surface roughness and thickness of the screen-printed electrodes were characterized using a Filmetrics® Profilm3D® Optical Profilometer. The device is based on white light interferometry. In white light interferometry, a white (or broad spectrum), spatially coherent light source is pointed at a beam splitter, which splits the incoming beam in half. Half of the light passes through the beam splitter onto a reference mirror, and half of the light is reflected at a 90° angle onto the measured object. The distance of the reference mirror from the beam splitter is adjustable. By correctly adjusting the distance within a range of a few micrometers, an interference pattern is created when the beams are recombined by the beam splitter at return and can be observed by the camera. The interference pattern contains information about the distance of the points on the measured object from the beam splitter and can be used to create a scan of the surface roughness of the sample. An illustration of the system is shown in figure 2.5. Results are discussed in section 3.1.3.

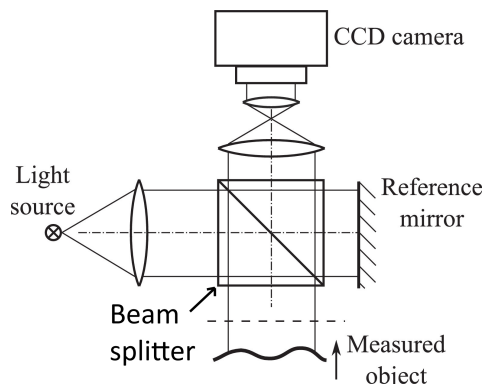


Figure 2.5: Illustration of white light interferometry based optical profilometry. Light beam is pointed at beam splitter, reflected by reference mirror and measured object and creates interference pattern when recombined. [40]

2.5 Test setup

2.5.1 Design and assembly

In order to conduct the experiments, a device similar to a Franz-Diffusion-cell was needed that brings the Strat-M® in contact with the artificial sweat solution on one side and distilled water on the other side. The exposed pads of the electrodes have to be uncovered to allow connecting a source meter such that a current can be applied. The source meter

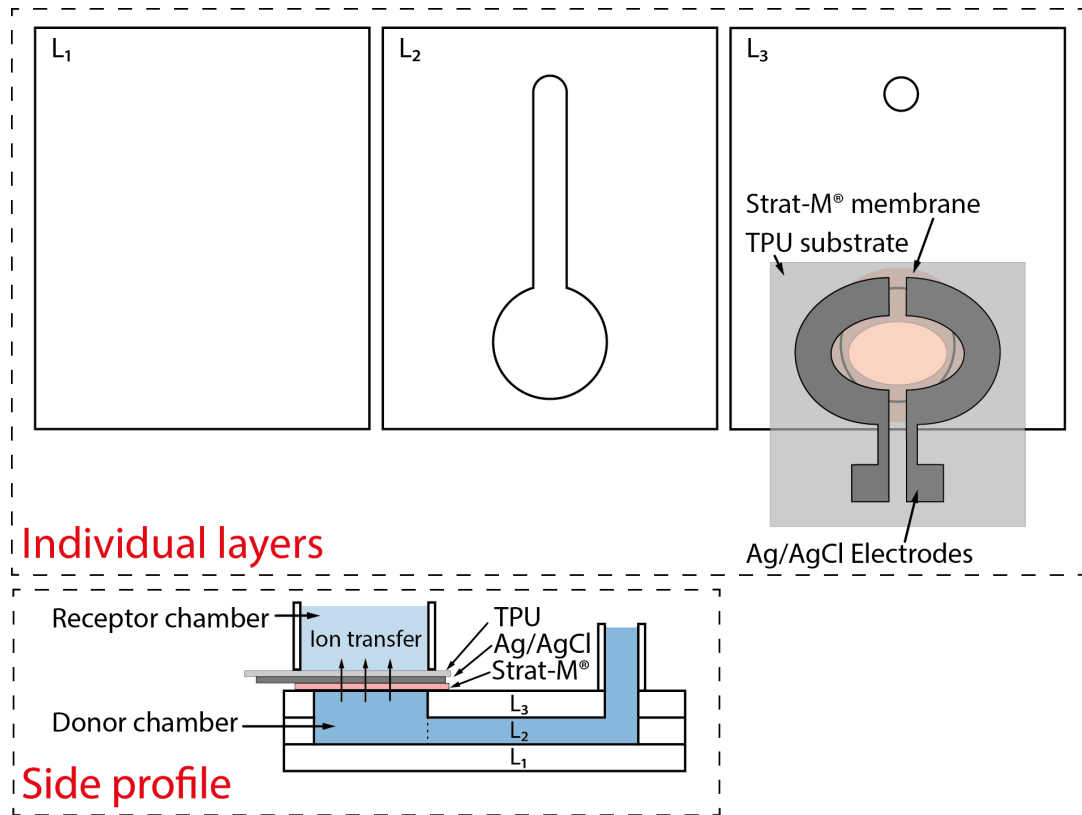


Figure 2.6: Layer by layer and side profile illustrations of design for testing device. L₁=base layer, L₂=channel from donor chamber to reservoir, L₃=cover for channel

used for experiments was the Keithley 2602B source meter. Figure 2.6 shows the final design layer by layer and as a side profile. L₁ is the base layer to which the other layers are glued. L₂ contains a circular cutout for the donor chamber and a small channel that leads to a reservoir. L₃ also has a cutout for the donor chamber and a small cutout at the end of the channel, but the channel is covered from the top. Above the smaller cutout at the end of the channel, a reservoir is placed, sitting at a higher level than the Strat-M® membrane, which puts the contained solution at a higher pressure and ensures that it is in contact with the membrane throughout the entire experiment. The three layers of the test device were cut from acrylic using a laser cutter and glued together using Loctite® Super Attak adhesive.

2.5.2 Procedure

The donor chamber of the device is filled with artificial sweat until the level reaches the top of the donor chamber cutout of L₃. The Strat-M® is carefully placed on top of the cutout while avoiding trapped air bubbles. The elliptical areas of the Ag/AgCl electrodes are covered with an electrolyte gel (Axion Elektroden Kontaktgel), which ensures good contact between the electrodes and the membrane. The Ag/AgCl electrodes are then

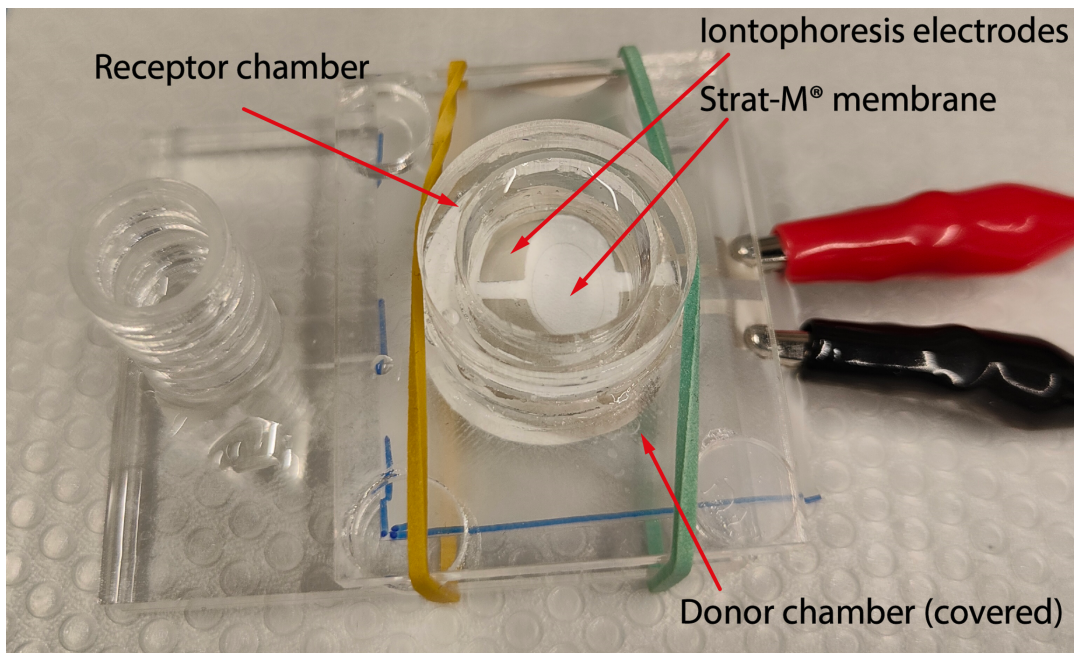


Figure 2.7: Assembled testing device with Strat-M® membrane and Ag/AgCl electrodes.

placed on top of the membrane. The receptor chamber is placed on top of the electrodes and secured with elastic bands. The force applied by the elastic bands ensures that the solution in the receptor chamber of the device does not leak from the sides. The receptor chamber is then filled with distilled water and the donor chamber is filled up to the top from the reservoir on the opposite side of the channel in L₂. Filling it to the top ensures that the donor chamber is under pressure and the membrane is always in contact with the solution. The assembled device is shown in figure 2.7. For each experiment, a constant current is applied by a source meter. 60 μ L samples are taken at regular time intervals from the solution in the receptor chamber using a micropipette. These samples are placed in the form of a drop on the sensing electrode connected to a potentiostat (PalmSens 4) which analyzes them using cyclic voltammetry, as described in section 2.6.1.

2.6 Monitoring ionic permeation through synthetic membrane

2.6.1 Cyclic voltammetry

To effectively characterize ion permeation during iontophoresis, electrochemical techniques are particularly well-suited for monitoring ionic permeation through the Strat-M® membrane from the donor to the receptor compartment. Among the available electrochemical platforms, three-electrode systems are commonly employed due to their ability to provide accurate and well-controlled measurements. In such systems, changes in analyte concentration are detected by the working electrode (WE) by measuring its potential rela-

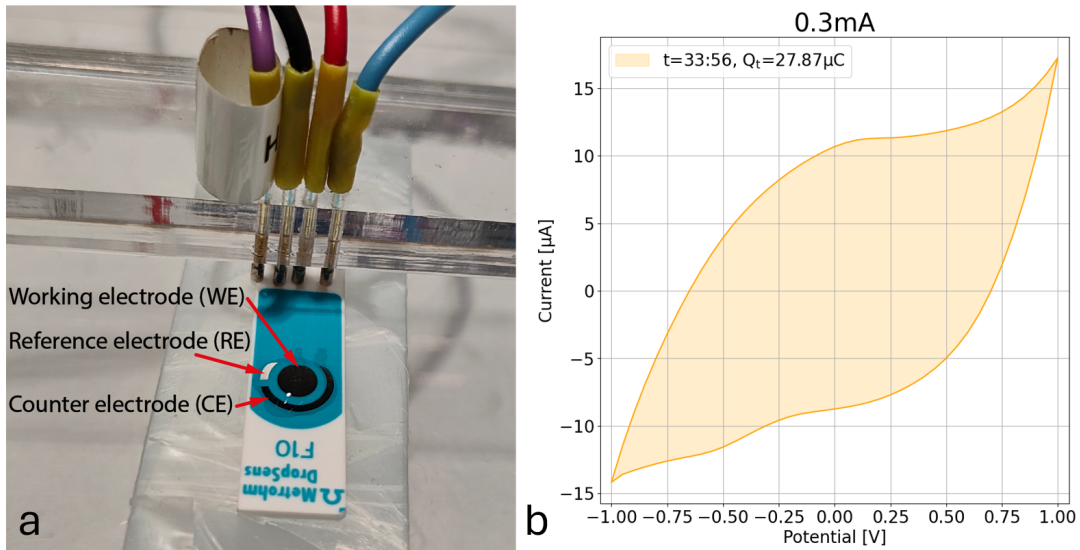


Figure 2.8: (a) Sensing electrodes connected to potentiostat (PalmSens4) used for cyclic voltammetry measurements (Metrohm DropSens F10); (b) Example of cyclic voltammogram recorded after applying iontophoresis current of 0.3mA for 33 minutes to the Strat-M® membrane.

tive to a stable reference electrode (RE) [41, 42]. The counter electrode (CE) completes the electrical circuit and facilitates current flow, allowing the RE to maintain a constant potential. In our experiments, a Metrohm DropSens F10, shown in figure 2.8(a) was used to carry out the measurements. In this electrode, the WE and CE are made of carbon, and the RE is made of Ag/AgCl. The three-electrode platform is frequently combined with cyclic voltammetry (CV) measurements to characterize electrochemical processes with high sensitivity and specificity [6, 12, 42]. A varying potential is applied to the WE and measured with respect to the RE, which maintains a constant potential. First, the potential is ramped up from a minimum to a maximum value and then ramped back to the minimum value, creating a triangular waveform [43]. Important parameters for this type of measurement are the minimum and maximum applied potential [V], the potential step (difference between each individual applied potential) [V], the scan rate (the rate at which the applied potential is increased or decreased) [$\frac{V}{s}$] and the number of scans. This cycling of the potential is repeated multiple times, which gives the technique its name: cyclic voltammetry. The current flowing through the WE is measured as a function of the applied potential. The current is then plotted against the applied potential, resulting in a cyclic voltammogram. An example of a cyclic voltammogram that was recorded during the experiments is shown in figure 2.8(b). The shape of the cyclic voltammogram, specifically the presence of peak currents at certain potentials, can provide insight into the electrochemical properties of the material being studied. The presence of redox-active ions leads to the appearance of current peaks at specific potentials. The peak current, i_p , can be

calculated using the Randles–Ševčík equation [44]:

$$i_p = (2.69 \times 10^5) \cdot n^{3/2} \cdot A \cdot D^{1/2} \cdot C \cdot v^{1/2}$$

where i_p is the peak current [A], n is the number of electrons transferred, A is the electrode area [cm^2], D is the diffusion coefficient [cm^2/s], C is the concentration of the analyte [$\frac{mol}{cm^3}$], and v is the scan rate. In our case, the analysis of these current peaks is not relevant because the solution we used in the donor chamber (artificial sweat) does not contain redox-active compounds. Instead, we analyzed the change in area enclosed by the cyclic voltammogram, also referred to as the total charge transferred, and hereafter denoted as Q_t . Q_t is calculated by integrating the measured current through the WE. Q_t is proportional to the conductivity of the solution. Initially, the solution in the receptor chamber is distilled water and is not conductive. Over time, as ions are transferred through the membrane, the solution becomes increasingly conductive. Q_t can therefore serve as a measure for the ions that have been transferred through the membrane. The Python code used for analyzing and plotting Q_t was developed for this thesis and is available at [45].

2.6.2 Parameters for cyclic voltammetry

For every experiment, a constant current was applied to the iontophoresis electrodes. The used current intensities were 0.1, 0.2, and 0.3 mA. For every value of applied current, 60 μL samples were taken from the receptor chamber in 5-minute intervals for 30 minutes and analyzed using cyclic voltammetry. The first cyclic voltammogram was deleted for every sample. The parameters for the PalmSens4 potentiostat were:

- E vertex1 (minimum potential): -1.0 V
- E vertex2 (maximum potential): 1.0 V
- E step (difference in potential between measurements): 0.05 V
- Scan rate (rate at which the potential is ramped): 0.1 V/s
- Number of scans: 5

3

Results

3.1 Performance evaluation of screen-printed Ag/AgCl electrodes on TPU substrate

3.1.1 Sheet resistance

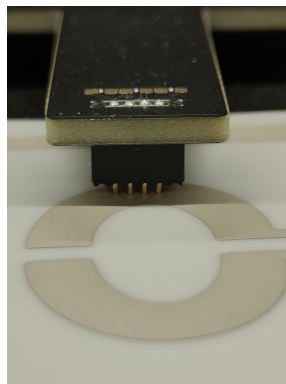


Figure 3.1: Ossila Four-Point Probe for sheet resistance measurements.

For each fabricated electrode, the sheet resistance was measured 100 times using the Ossila Four-Point Probe described in section 2.4.2 and shown in figure 3.1. From these measurements, the mean and standard deviation were computed per electrode. To evaluate the overall stability of the screen printing process, the mean sheet resistance of each electrode was used to calculate the global average ($44.47 \frac{m\Omega}{sq}$) and its standard deviation between electrodes ($10.57 \frac{m\Omega}{sq}$). Furthermore, the average standard deviation of the individual electrodes ($3.70 \frac{m\Omega}{sq}$) was calculated to assess the measurement precision of the Four-Point Probe device. During the first experiments, a current of 1 mA was applied with a source meter. The thin threads of the electrodes overheated and were destroyed, which limited the current intensity that could be applied in further experiments. In future designs, this can be avoided by increasing the width of the connections from

the exposed pads to the elliptical electrodes. Figure 3.2(a) shows the resulting damage. During prolonged experiments, the anode showed signs of corrosion, shown in figure 3.2(b).

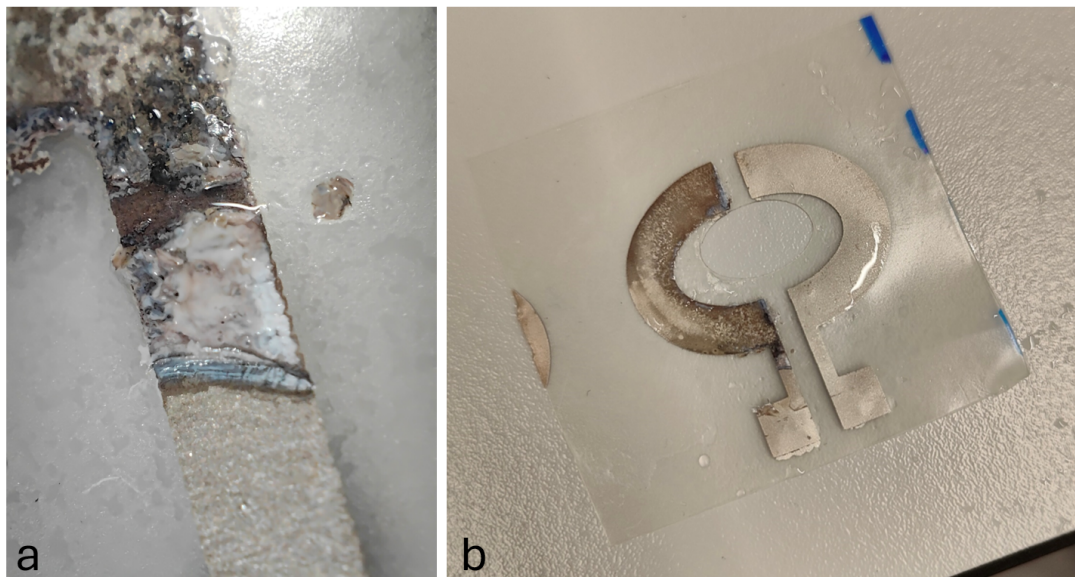


Figure 3.2: Overview of different types of degradation of iontophoresis electrodes. (a) Burned connection from exposed pad to elliptical electrode due to excessive current; (b) Corroded anode of iontophoresis electrodes.

3.1.2 Visual inspection with microscope

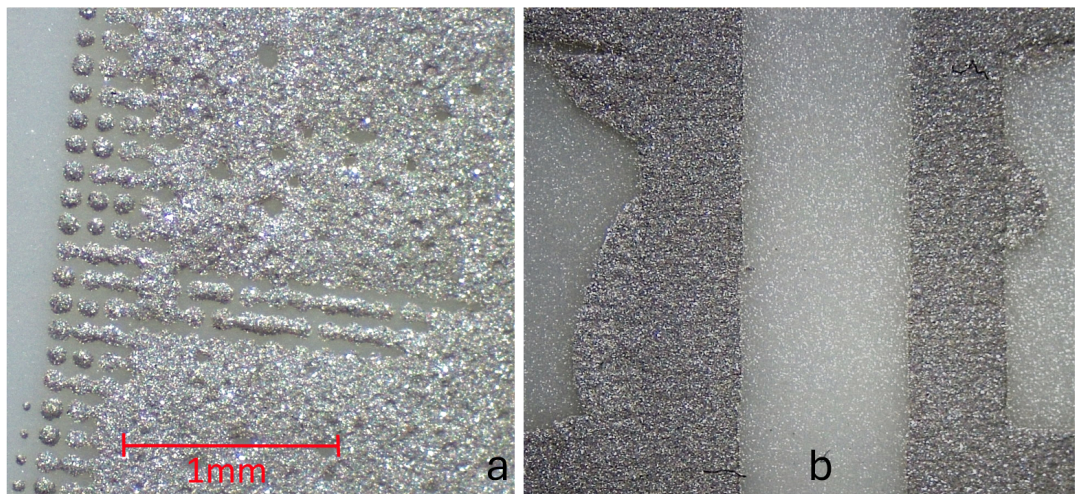


Figure 3.3: Visual inspection of screen-printed electrodes under microscope. (a) Screen-printed Ag/AgCl electrodes with incomplete surface coating due to insufficient ink; (b) Ink spill outside of intended shape on screen-printed electrodes due to degradation of vinyl mask;

When inspecting the electrodes under an optical microscope, two types of defects were visible, caused by different errors in the screen printing process. The first type of defect is caused by a lack of ink, leading to incomplete coverage of the electrode area on the substrate, shown in figure 3.3(a). Ink permeates through the individual pores of the screen, but the amount of ink is not sufficient to create a continuous print. This results in areas where the electrode is not fully formed, leading to highly reduced or no conductivity in those regions. The second type of defect was caused by the degradation of the vinyl mask. The degradation is caused by the friction of the squeegees pressing against the mask at every iteration of the printing process. This degradation leads to ink spilling outside the intended shape, shown in figure 3.3(b). These defects can be avoided by making sure that the amount of ink is sufficient for a complete coating of the electrode shape and replacing the vinyl mask before excessive degradation. An example of screen-printed electrodes with high-quality surface coating is shown in figure 3.4.



Figure 3.4: Screen printed Ag/AgCl electrodes with high quality surface coating.

3.1.3 Evaluation of surface roughness with optical profilometer

Figure 3.5(a) shows a top view of the optical-profilometric scan that was taken using the Profilm3D® device described in section 2.4.3. The size of the scanned area is $1000\mu\text{m} \times 800\mu\text{m}$. The scan shows peaks in material deposition at a thickness of $11\mu\text{m}$ and valleys at a thickness of $1\mu\text{m}$. It should be noted that the scan was taken at the edge of the printed electrode where the surface is generally rougher due to the nature of the screen printing process. A measure that could be taken to decrease the surface roughness of the screen-printed electrodes in future iterations is to use a screen with a higher mesh count.

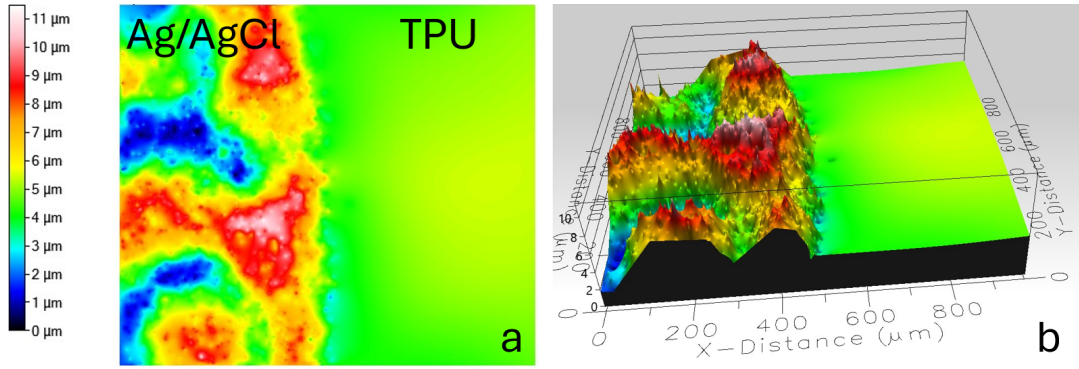


Figure 3.5: Optical profilometry scan of $1000\mu\text{m} \times 800\mu\text{m}$ area. (a) Top view (2d) shows peaks of $11\mu\text{m}$ and valleys of $1\mu\text{m}$ Ag/AgCl thickness; (b) 3d-rendering of optical profilometric scan.

3.2 Determination of current intensity for optimal ion transfer

3.2.1 Processing of measurements

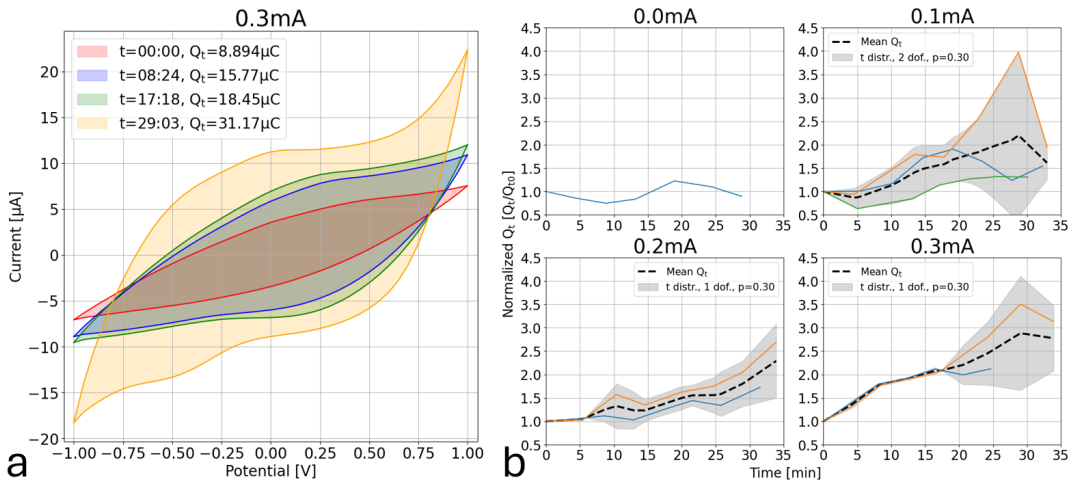


Figure 3.6: Overview of data processing. (a) Q_t at different time intervals for applied current intensity 0.3 mA; (b) Relative changes in Q_t for various applied current intensities and multiple experiments, average relative change of Q_t , and confidence interval. [45]

The data obtained through cyclic voltammetry measurements was analyzed. Because of the solution that was used in the donor chamber (artificial sweat), the analysis of peak currents was not relevant because there were no redox-active compounds present. For every sample, the cyclic voltammograms obtained were averaged, and the area enclosed by the average curve was normalized with respect to its value measured at 0 minutes. Figure 3.6(a) shows the averaged cyclic voltammograms at different time intervals for an applied current of 0.3 mA. The relative change in Q_t for different current intensities and multiple experiments, including the average relative change, was plotted against

time, shown in figure 3.6(b). The confidence interval for a p-value of 0.3 was plotted for measurements that follow a Student's t distribution. The relative changes in Q_t were interpolated linearly and extrapolated where necessary (when the end times did not match) to compute the average relative change in Q_t , which shows a clear trend for all applied current intensities. The average relative changes in Q_t for all applied current intensities are plotted separately in figure 3.7.

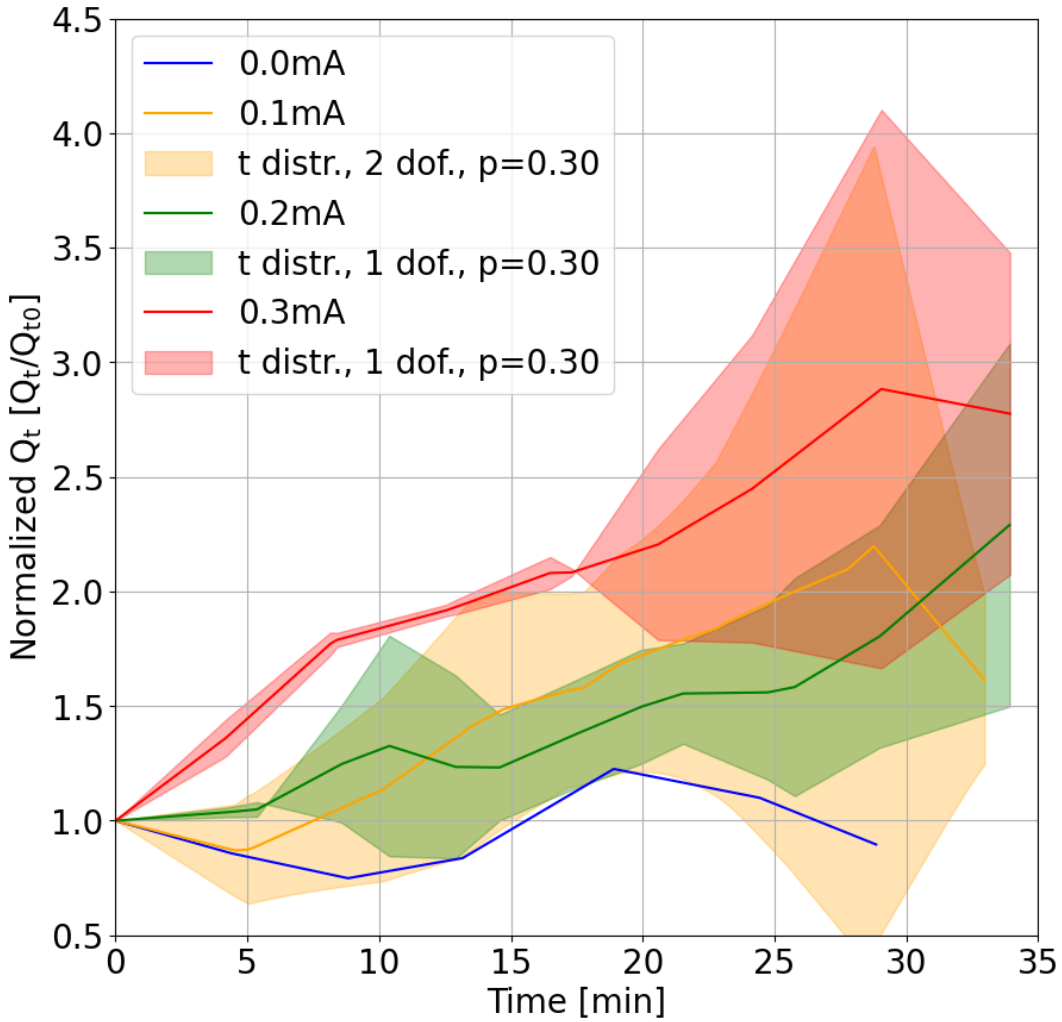


Figure 3.7: Average relative change in Q_t over time for current intensities (0.1, 0.2, 0.3) mA including confidence interval for Student's t distribution with p-value of 0.3. Clear correlation between current intensity and change in Q_t is visible. [45]

3.2.2 Analysis of measurements

From the previous figures, several observations can be made regarding the behavior of ion transfer across the membrane under different current intensities. Most notably, the results indicate a clear correlation between the applied current and the rate of ion transfer. As the

applied current increases, the relative change in Q_t per unit time also increases, signifying a higher rate of ion transfer across the membrane. Through these measurements, it was confirmed that within the range of currents applied, the highest rate of ion transfer was achieved with a current intensity of 0.3 mA, but there was no sign of diminishing returns while increasing the current. The current of 0.3 mA is also well below the perception threshold [46]. Additionally, it can be observed that when no current was applied, there was no measurable change in Q_t over time, and therefore, no ion transfer occurred. This confirms that passive diffusion through the membrane is negligible under the conditions of these experiments, and that an iontophoretic current is necessary to achieve ion migration. The confidence intervals plotted in the graphs are calculated for a relatively high p-value (0.3), but still suggest that the observed differences in Q_t values are systematic and not due to random variation, especially at higher current levels.

4

Conclusion

This thesis successfully demonstrated the design, fabrication, and testing of a screen-printed DC system for iontophoretic sweat extraction, aimed at applications in wearable biosensing devices. By leveraging TPU as a flexible substrate and Ag/AgCl as the material for the screen printed iontophoresis electrodes, a functional and skin-conforming electrode system was developed. The fabricated electrodes showed consistent performance, as confirmed by four-point probe measurements. The quality of the surface coating obtained through screen printing was confirmed by visual inspection with an optical microscope and optical profilometry. The integration of the Strat-M® synthetic membrane as a substitute for skin allowed for the safe and repeatable testing of iontophoresis without involving human subjects. The developed test platform, using artificial sweat and cyclic voltammetry analysis, confirmed effective ion transfer under various applied currents, while confirming the correlation between ion transfer and applied iontophoresis current. The highest achieved rate of ion transfer across the membrane was obtained with an applied current intensity of 0.3 mA. It was shown that the rate of ion transfer consistently increases as the iontophoresis current is increased, and that when no current was applied, ion transfer through the membrane was negligible. These findings validate the feasibility of this low-cost, flexible system for controlled, on-demand sweat extraction—paving the way for future integration into wearable biosensing platforms. Compared to the existing literature, experiments were conducted specifically to assess the correlation between ion transfer through a synthetic membrane under iontophoretic conditions. Further work may focus on conducting *in vivo* testing to assess real-world performance for sweat extraction. Nonetheless, this study lays a foundation for the development of non-invasive biosensing devices for continuous health monitoring.

Bibliography

- [1] Jayoung Kim, Alan S. Campbell, Berta Esteban-Fernández de Ávila, and Joseph Wang. "Wearable biosensors for healthcare monitoring". In: *Nature Biotechnology* 37.4 (2019), pp. 389–406.
- [2] Tucker Stuart, Jessica Hanna, and Philipp Gutruf. "Wearable devices for continuous monitoring of biosignals: Challenges and opportunities". en. In: *APL Bioeng* 6.2 (Apr. 2022), p. 021502.
- [3] Haixia Yu and Jintao Sun. "Sweat detection theory and fluid driven methods: A review". In: *Nanotechnology and Precision Engineering* 3.3 (2020), pp. 126–140.
- [4] Fupeng Gao, Chunxiu Liu, Lichao Zhang, Tiezhu Liu, Zheng Wang, Zixuan Song, Haoyuan Cai, Zhen Fang, Jiamin Chen, Junbo Wang, Mengdi Han, Jun Wang, Kai Lin, Ruoyong Wang, Mingxiao Li, Qian Mei, Xibo Ma, Shuli Liang, Guangyang Gou, and Ning Xue. "Wearable and flexible electrochemical sensors for sweat analysis: a review". In: *Microsystems & Nanoengineering* 9.1 (2023), p. 1.
- [5] Mattia Petrelli, Ata Golparvar, Ali Meimandi, Bajramshahe Shkodra, Martina Aurora Costa Angeli, Aniello Falco, Paolo Lugli, Luisa Petti, and Sandro Carrara. "Flexible Sensor and Readout Circuitry for Continuous Ion Sensing in Sweat". In: *IEEE Sensors Letters* 7.6 (2023), pp. 1–4.
- [6] Moritz Ploner, Mattia Petrelli, Bajramshahe Shkodra, Anna Tagliaferri, Paolo Lugli, Daniele Resnati, Luisa Petti, and Martina Aurora Costa Angeli. "A comprehensive review on electrochemical cytokine detection in sweat". In: *Cell Reports Physical Science* (2024).
- [7] Christopher Legner, Upender Kalwa, Vishal Patel, Austin Chesmore, and Santosh Pandey. "Sweat sensing in the smart wearables era: Towards integrative, multi-functional and body-compliant perspiration analysis". In: *Sensors and Actuators A: Physical* 296 (2019), pp. 200–221.
- [8] Moritz Ploner, Bajramshahe Shkodra, Antonio Altana, Mattia Petrelli, Anna Tagliaferri, Daniele Resnati, Paolo Lugli, Martina Aurora Costa Angeli, and Luisa Petti. "Flexible Electrochemical Sensor for Interleukin-6: Toward Wearable Cytokine Monitoring". In: *IEEE Sensors Letters* 8.8 (2024), pp. 1–4.
- [9] Jinmyeong Kim, Seungwoo Noh, Jeong Ah Park, Sang-Chan Park, Seong Jun Park, Jin-Ho Lee, Jae-Hyuk Ahn, and Taek Lee. "Recent advances in aptasensor for cytokine detection: A review". In: *Sensors* 21.24 (2021), p. 8491.
- [10] Manpreet Singh, Johnson Truong, W Brian Reeves, and Jong-in Hahm. "Emerging cytokine biosensors with optical detection modalities and nanomaterial-enabled signal enhancement". In: *Sensors* 17.2 (2017), p. 428.

- [11] Weiyi Liu, Huanyu Cheng, and Xiufeng Wang. "Skin-interfaced colorimetric microfluidic devices for on-demand sweat analysis". In: *npj Flexible Electronics* 7.1 (2023), p. 43.
- [12] M Ploner, B Shkodra, L Franchin, A Altana, M Petrelli, MA Costa Angeli, G Ciccone, T Antrack, L Vanzetti, RR Nair, et al. "Flexible Microfluidics-Integrated Electrochemical System for Detection of Tumor Necrosis Factor-Alpha Under Continuous Flow of Sweat". In: *Biosensors and Bioelectronics* (2025), p. 117734.
- [13] Bajramshahe Shkodra, Biresaw Demelash Abera, Giuseppe Cantarella, Ali Douaki, Enrico Avancini, Luisa Petti, and Paolo Lugli. "Flexible and printed electrochemical immunosensor coated with oxygen plasma treated SWCNTs for histamine detection". In: *Biosensors* 10.4 (2020), p. 35.
- [14] Antonio Altana, Bajramshahe Shkodra, Pietro Ibba, Martina Aurora Costa Angeli, Moritz Ploner, Mattia Petrelli, Eva-Maria Korek, Paolo Lugli, and Luisa Petti. "Textile-Integrated Organic Electrochemical Transistor for Selective Ion Detection via Electrical Impedance Spectroscopy". In: *IEEE Sensors Letters* (2024).
- [15] Lindsay B Baker. "Physiology of sweat gland function: The roles of sweating and sweat composition in human health". en. In: *Temperature (Austin)* 6.3 (July 2019), pp. 211–259.
- [16] Xichen Yuan, Chen Li, Xu Yin, Yang Yang, Bowen Ji, Yinbo Niu, and Li Ren. "Epidermal Wearable Biosensors for Monitoring Biomarkers of Chronic Disease in Sweat". In: *Biosensors* 13.3 (2023).
- [17] Sam Emaminejad, Wei Gao, Eric Wu, Zoe A. Davies, Hnin Yin Yin Nyein, Samyuktha Challa, Sean P. Ryan, Hossain M. Fahad, Kevin Chen, Ziba Shahpar, Salmonn Talebi, Carlos Milla, Ali Javey, and Ronald W. Davis. "Autonomous sweat extraction and analysis applied to cystic fibrosis and glucose monitoring using a fully integrated wearable platform". In: *Proceedings of the National Academy of Sciences* 114.18 (2017), pp. 4625–4630. eprint: <https://www.pnas.org/doi/pdf/10.1073/pnas.1701740114>.
- [18] A Mena-Bravo and M D Luque de Castro. "Sweat: a sample with limited present applications and promising future in metabolomics". en. In: *J Pharm Biomed Anal* 90 (Dec. 2013), pp. 139–147.
- [19] Phillip Simmers, S. Kevin Li, Gerald Kasting, and Jason Heikenfeld. "Prolonged and localized sweat stimulation by iontophoretic delivery of the slowly-metabolized cholinergic agent carbachol". In: *Journal of Dermatological Science* 89.1 (2018), pp. 40–51.

- [20] Sarah A Molokhia, Yanhui Zhang, William I Higuchi, and S Kevin Li. "Iontophoretic transport across a multiple membrane system". en. In: *J Pharm Sci* 97.1 (Jan. 2008), pp. 490–505.
- [21] Nur Fatin Adini Ibrahim, Norhayati Sabani, Shazlina Johari, Asrulnizam Abd Manaf, Asnida Abdul Wahab, Zulkarnay Zakaria, and Anas Mohd Noor. "A Comprehensive Review of the Recent Developments in Wearable Sweat-Sensing Devices". en. In: *Sensors (Basel)* 22.19 (Oct. 2022).
- [22] Kiran Peringeth, Anindita Ganguly, Arnab Pal, Jaba Roy Chowdhury, Kuldeep Kaswan, Hsuan-Yu Ho, Jui-Han Yu, Fu-Cheng Kao, and Zong-Hong Lin. "Self-powered microfluidic-based sensor for noninvasive sweat analysis". In: *Sensors and Actuators B: Chemical* 423 (2025), p. 136859.
- [23] Hnin Yin Yin Nyein, Mallika Bariya, Liisa Kivimäki, Sanna Uusitalo, Tiffany Sun Liaw, Elina Jansson, Christine Heera Ahn, John A. Hangasky, Jiangqi Zhao, Yuanjing Lin, Tuomas Happonen, Minghan Chao, Christina Liedert, Yingbo Zhao, Li-Chia Tai, Jussi Hiltunen, and Ali Javey. "Regional and correlative sweat analysis using high-throughput microfluidic sensing patches toward decoding sweat". In: *Science Advances* 5.8 (2019), eaaw9906. eprint: <https://www.science.org/doi/pdf/10.1126/sciadv.aaw9906>.
- [24] Jayoung Kim, Julianne R Sempionatto, Somayeh Imani, Martin C Hartel, Abbas Barfidokht, Guangda Tang, Alan S Campbell, Patrick P Mercier, and Joseph Wang. "Simultaneous Monitoring of Sweat and Interstitial Fluid Using a Single Wearable Biosensor Platform". en. In: *Adv Sci (Weinh)* 5.10 (Aug. 2018), p. 1800880.
- [25] Jayoung Kim, Itthipon Jeerapan, Somayeh Imani, Thomas N. Cho, Amay Bandodkar, Stefano Cinti, Patrick P. Mercier, and Joseph Wang. "Noninvasive Alcohol Monitoring Using a Wearable Tattoo-Based Iontophoretic-Biosensing System". In: *ACS Sensors* 1.8 (2016), pp. 1011–1019.
- [26] Robert P Hirten, Kai-Chun Lin, Jessica Whang, Sarah Shahub, Drew Helmus, Sriram Muthukumar, Bruce E Sands, and Shalini Prasad. "Longitudinal assessment of sweat-based TNF-alpha in inflammatory bowel disease using a wearable device". en. In: *Sci Rep* 14.1 (Feb. 2024), p. 2833.
- [27] Sarah Shahub, Annapoorna Ramasubramanya, Preeti Singh, Ruchita Mahesh Kumar, Kai-Chun Lin, Sriram Muthukumar, and Shalini Prasad. "Longitudinal tracking of chronic inflammation through Calprotectin and Interleukin-6 using a sweat wearable device". In: *Biosensors and Bioelectronics: X* 24 (2025), p. 100622.
- [28] Dan-In Jang, A-Hyeon Lee, Hye-Yoon Shin, Hyo-Ryeong Song, Jong-Hwi Park, Tae-Bong Kang, Sang-Ryong Lee, and Seung-Hoon Yang. "The Role of Tumor Necrosis

- Factor Alpha (TNF- α) in Autoimmune Disease and Current TNF- α Inhibitors in Therapeutics". en. In: *Int J Mol Sci* 22.5 (Mar. 2021).
- [29] Andrea Marques-Deak, Giovanni Cizza, Farideh Eskandari, Sara Torvik, Israel C Christie, Esther M Sternberg, Terry M Phillips, For the POWER, and Study Group. "Measurement of cytokines in sweat patches and plasma in healthy women: validation in a controlled study". In: *Journal of immunological methods* 315.1-2 (2006), pp. 99–109.
- [30] Sílvia Manuela Ferreira Cruz, Luís A. Rocha, and Júlio C. Viana. "Printing Technologies on Flexible Substrates for Printed Electronics". In: *Flexible Electronics*. Ed. by Simas Rackauskas. Rijeka: IntechOpen, 2018. Chap. 3.
- [31] Huiqing Zhang, Rongyan He, Hao Liu, Yan Niu, Zedong Li, Fei Han, Jing Li, Xiongwen Zhang, and Feng Xu. "A fully integrated wearable electronic device with breathable and washable properties for long-term health monitoring". In: *Sensors and Actuators A: Physical* 322 (2021), p. 112611.
- [32] Hyeonseok Kim, Eugene Kim, Chanyeong Choi, and Woon-Hong Yeo. "Advances in Soft and Dry Electrodes for Wearable Health Monitoring Devices". en. In: *Micro-machines (Basel)* 13.4 (Apr. 2022).
- [33] Huibao Chen, Yafei Ding, Guimei Zhu, Yu Liu, Qun Fang, Xue Bai, Yan Zhao, Xin Li, Xingyi Huang, Tong-Yi Zhang, Baowen Li, and Bin Sun. "A new route to fabricate flexible, breathable composites with advanced thermal management capability for wearable electronics". In: *npj Flexible Electronics* 7.1 (2023), p. 24.
- [34] Tae Woog Kang, Jimin Lee, Youngjin Kwon, Yoon Jae Lee, and Woon-Hong Yeo. "Recent Progress in the Development of Flexible Wearable Electrodes for Electrocardiogram Monitoring During Exercise". In: *Advanced NanoBiomed Research* 4.8 (2024), p. 2300169. eprint: <https://advanced.onlinelibrary.wiley.com/doi/pdf/10.1002/anbr.202300169>.
- [35] Mattia Petrelli, Bajramshahe Shkodra, Aniello Falco, Martina Aurora Costa Angeli, Sahira Vasquez, Alessandra Scarton, Silvia Pogliaghi, Roberto Biasi, Paolo Lugli, and Luisa Petti. "Method for instability compensation and detection of ammonium in sweat via conformal electrolyte-gated field-effect transistors". In: *Organic Electronics* 122 (2023), p. 106889.
- [36] Takashi Uchida, Wesam R. Kadhum, Sayumi Kanai, Hiroaki Todo, Takeshi Oshizaka, and Kenji Sugibayashi. "Prediction of skin permeation by chemical compounds using the artificial membrane, Strat-M™". In: *European Journal of Pharmaceutical Sciences* 67 (2015), pp. 113–118.

- [37] SBCCOE. "Gross Anatomy of the Integumentary System". In: *Anatomy & Physiology* (2025). eprint: <https://pressbooks.ccconline.org/bio106/chapter/integumentary-structures-and-functions/>.
- [38] Anika Haq, Mania Dorrani, Benjamin Goodyear, Vivek Joshi, and Bozena Michniak-Kohn. "Membrane properties for permeability testing: Skin versus synthetic membranes". In: *International Journal of Pharmaceutics* 539.1 (2018), pp. 58–64.
- [39] Almudena Rivadeneyra, Florin C. Loghin, and Aniello Falco. "Technological Integration in Printed Electronics". In: *Flexible Electronics*. Ed. by Simas Rackauskas. Rijeka: IntechOpen, 2018. Chap. 5.
- [40] Pavel Pavliček and Erik Mikeska. "White-light interferometer without mechanical scanning". In: *Optics and Lasers in Engineering* 124 (2020), p. 105800.
- [41] Samar Damiati and Bernhard Schuster. "Electrochemical biosensors based on S-layer proteins". In: *Sensors* 20.6 (2020), p. 1721.
- [42] Nirmita Dutta, Peter B Lillehoj, Pedro Estrela, and Gorachand Dutta. "Electrochemical biosensors for cytokine profiling: Recent advancements and possibilities in the near future". In: *Biosensors* 11.3 (2021), p. 94.
- [43] V. Climent and J.M. Feliu. "Cyclic Voltammetry". In: *Encyclopedia of Interfacial Chemistry*. Ed. by Klaus Wandelt. Oxford: Elsevier, 2018, pp. 48–74.
- [44] Noémie Elgrishi, Kelley J. Rountree, Brian D. McCarthy, Eric S. Rountree, Thomas T. Eisenhart, and Jillian L. Dempsey. "A Practical Beginner's Guide to Cyclic Voltammetry". In: *Journal of Chemical Education* 95.2 (2018), pp. 197–206.
- [45] Benjamin Schmid Ties. *Jupyter Notebook for analyzing cyclic voltammetry data from PSTrace software*. eprint: https://github.com/benjibst/cyclic_voltammetry_notebook.
- [46] Raymond M Fish and Leslie A Geddes. "Conduction of electrical current to and through the human body: a review". en. In: *Eplasty* 9 (Oct. 2009), e44.